Earth's Future

RESEARCH ARTICLE
10.1029/2025EF007833

Future Changes to Rainfall Extremes Over Puerto Rico in a Convection-Permitting Model

E. M. Dougherty[1], **A. F. Prein**[2], **and P. A. O'Gorman**[3]

[1]Research Applications Lab, NSF National Center for Atmospheric Research, Boulder, CO, USA, [2]Institute for Atmospheric and Climate Science, ETH Zürich, Zürich, Switzerland, [3]Department of Earth, Atmospheric and Planetary Sciences, Massachussets Institue of Technology, Cambridge, MA, USA

Key Points:

- Future changes to rainfall extremes over Puerto Rico are simulated in a global model at convection-permitting scale over the Caribbean
- Extreme rainfall accumulations increase in the early rainy season but decrease in the late rainy season by mid-century
- These seasonal changes are related to differences in subsidence, island convergence, and updraft velocity

Supporting Information:

Supporting Information may be found in the online version of this article.

Correspondence to:

E. M. Dougherty,
doughert@ucar.edu

Citation:

Dougherty, E. M., Prein, A. F., & O'Gorman, P. A. (2026). Future changes to rainfall extremes over Puerto Rico in a convection-permitting model. *Earth's Future*, *14*, e2025EF007833. https://doi.org/10.1029/2025EF007833

Received 1 DEC 2025
Accepted 11 APR 2026

Abstract Islands in the Caribbean are vulnerable to anthropogenic warming due to sea level rise and their reliance on rainfall for agriculture. These islands are particularly prone to rainfall extremes, such as the 1,029 mm of daily maximum rain in Puerto Rico due to Hurricane Maria in 2017. Rainfall extremes mostly occur in the early rainy season (ERS) from April–June and late rainy season (LRS) from August–November. While global climate models project reduced rainfall in the Caribbean by the end of the century, they are too coarse to properly resolve the complex coastline and terrain of Puerto Rico and associated convection that is often induced by sea-breeze convergence and orographic uplift. Here, we resolve this issue by running the Model for Prediction Across Scales-Atmosphere (MPAS-A) using a 60–3 km global variable mesh centered over the Caribbean to downscale extreme rainfall days from coarser transient simulations during 2001–2021 and 2041–2061. This model configuration allows for the evaluation of dynamical and thermodynamic future changes at convection-permitting scales over Puerto Rico using MESACLIP as forcing data, although these simulations underestimate extreme rainfall amounts. Results show that by mid-century, rainfall extremes increase in the ERS but decrease in the LRS, mainly associated with changes in isolated convection. Stronger upward motion and sea breeze convergence support future increased rainfall in the ERS, while stronger subsidence likely reduces LRS rainfall extremes. These results suggest that more attention needs to be given to the increasing risk of ERS rainfall extremes over Puerto Rico.

Plain Language Summary Puerto Rico is an island in the Caribbean that is vulnerable to the impacts of global warming due to sea level rise and its dependence on rainfall for agriculture. Most of the rainfall over the island falls from April–June and August–November due to thunderstorms initiated by the terrain and winds hitting the coastline, which cannot be resolved in coarser atmospheric models. We run an atmospheric model globally that resolves finer scales over Puerto Rico and the Caribbean to address this issue in order to understand changes to the most extreme rainfall by mid-century. We find that rainfall extremes increase in April–June and decrease in August–November, mainly due to changes in upward and downward motions as well as the winds converging along the coastline.

1. Introduction

1.1. Rainfall Drivers Over Puerto Rico

Puerto Rico is a Caribbean island that is particularly vulnerable to rainfall extremes and climate change (Archer et al., 2024; Thomas et al., 2019). One of the most extreme rainfall events to affect the island recently was Hurricane Maria in 2017 which resulted in the largest daily maximum rainfall of 1,029 mm at one station in the southeast region of the island (Keellings & Hernández Ayala, 2019) and was the third costliest natural disaster in U.S. history (Pasch et al., 2018). Tropical cyclones (TCs) generate much of the extreme flood events over Puerto Rico, with 51 out of 86 TCs passing near the island being associated with the 99th percentile of streamflow (Hernández Ayala et al., 2017). Furthermore, one third of the extreme discharge events in the United States and Puerto Rico occurs in Puerto Rico and Hawaii (O'Connor & Costa, 2004), illustrating that these are particularly flood-prone islands, especially once sea level rise is considered (Jury, 2018).

The rainfall in Puerto Rico mainly falls during its two distinct rainy seasons-an early rainy season (ERS) from mid April–mid June and a late rainy season (LRS) from late August–November (Martinez et al., 2019). The ERS and LRS are largely dictated by moisture convergence from the Intertropical Convergence Zone (ITCZ) and the North Atlantic Subtropical High (NASH). During the ERS, convergence is induced as the western flank of the NASH

expands westward and the ITCZ migrates northward. In the mid-summer dry period, the NASH extends further west, and subsidence and dry air advection associated with the trades return. In the LRS, the NASH contracts eastward and its western flank and associated moisture convergence returns to the central Caribbean. The El Niño Southern Oscillation also induces an indirect effect over Puerto Rico by changing the sea level pressure patterns, thus the NASH, winds, and sea surface temperatures (SSTs; Giannini et al., 2000, 2001a,b).

At the mesoscale, the complex terrain and sea breeze influence rainfall patterns over the island. An east-west mountain range, the Cordillera Central, and the northeast Luquillo Mountains influence the spatial rainfall distribution, with average rainfall of 4,346 mm yr^{-1} in the northeast and <745 mm yr^{-1} in the southwest (Bhardwaj et al., 2018; Hosannah et al., 2019). These mountain ranges interact with northeasterly trade winds and sea breezes to produce local convergence and rainfall over Puerto Rico (Hosannah et al., 2019; Jury & Chiao, 2013; Jury et al., 2009). Therefore, in addition to TCs, rainfall due to isolated convection and mesoscale convective systems (MCSs) are common (Jury et al., 2009; Prein et al., 2023).

1.2. Changes to Tropical Precipitation in GCMs

Future projections of rainfall changes over the Caribbean using global climate models (GCMs) mainly show a drying trend. The Coupled Model Intercomparison Project Phase 6 (CMIP6) shows a 10%–40% decrease in precipitation over the Caribbean (Almazroui et al., 2021; Herrera et al., 2020) and an average decrease of 0.2–0.5 mm day^{-1} under Radiative Concentration Pathway 8.5 (Brotons et al., 2024). The annual maximum precipitation is also projected to decrease over this region in CMIP5 by 2100, which is due to increased subsidence despite the increasing thermodynamic contribution from increased moisture (Pfahl et al., 2017). Brotons et al. (2024) attribute this future drying to strong future surface warming in the central/east Pacific (resembling El Niño) that drives an eastward migration and weakening of the Pacific Walker circulation that induces large-scale subsidence over the Caribbean.

While GCMs project a future drying trend over the Caribbean, they have large biases, especially related to precipitation as convection and islands (including their topography) are not resolved at their coarse (∼1°–2.5°) grid spacing (Campbell et al., 2021; Herrera et al., 2020; Jury, 2009; Martin & Schumacher, 2011). Caribbean precipitation is substantially underestimated in CMIP6 models (Brotons et al., 2024; Martinez et al., 2025), with a 55.7% underestimation over land (Brotons et al., 2024). Many CMIP6 models feature an "double-ITCZ" (Adam et al., 2018; Brotons et al., 2024; Zhang et al., 2015), SST biases (Martinez et al., 2025), and large biases in the ERS (Campbell et al., 2021; Martinez et al., 2025). Furthermore, Pfahl et al. (2017) show that uncertainties in extreme precipitation projections are largest over the tropics. Using higher resolution GCMs, such as those with <0.5° resolution like the simulations performed with the Community Earth System Model (Chang et al., 2020; Small et al., 2014), tend to show smaller biases (Martinez et al., 2025). This suggests using higher resolution models could provide a more robust estimate of extreme precipitation changes over Puerto Rico.

1.3. Convection-Permitting Simulations Over the Tropical Atlantic

Given the biases in GCMs, recent studies have utilized convection-permitting models (CPMs) that explicitly resolve convection and reduce precipitation biases (Kendon et al., 2014; Prein et al., 2015) to study changes over Puerto Rico and the tropics. CPMs are especially beneficial to simulate the weather of Puerto Rico given its small size and complex terrain, and the ability of CPMs to eliminate the double ITCZ bias (Heim et al., 2023; Núñez Ocasio & Dougherty, 2024). Bhardwaj et al. (2018) produced 20-year historic and 20-year future simulations over Puerto Rico at 2-km grid spacing by forcing the Japanese Meteorological Agency Non-Hydrostatic Model in the Regional Spectral Model with the Community Climate System Model. Akinsanola et al. (2024) produced non-continous 20-year historical simulations over the island at a 4-km grid spacing by downscaling the European Center for Medium Range Forecast Reanalysis v5 (ERA5) reanalysis data (Hersbach et al., 2020) with the Weather Research and Forecasting model. They showed that the 4-km model overestimates mean and extreme precipitation by ∼25%, which is still an improvement compared to ERA5, while Bhardwaj et al. (2018) shows a notable dry bias. By mid-century, mean rainfall is projected to decrease over Puerto Rico with a reduced frequency of extreme hourly rainfall, which Bhardwaj et al. (2018) attributes to increased subsidence and weakened orographic uplift.

CPMs in conjunction with the pseudo-global warming (PGW) method (Schär et al., 1996) have been used to investigate the impacts of a warmer and moister climate on historical TCs. Patricola and Wehner (2018) used this

Table 1
The Number of Extreme Rainfall Cases Simulated in MPAS-A in the Historical and Future Climate, as Well as the Early Rainy Season and Late Rainy Season

	Historical	Future	Total
Early rainy season (Apr-June)	27	27	54
Late rainy season (Aug-Nov)	36	36	72
Total	63	63	126

method to show a projected 2%–30% increase in TC rainfall due to warming under RCP8.5. For 22 TCs in the western Atlantic, Gutmann et al. (2018) also used a 13-year CPM with the PGW method and found TCs had faster maximum winds, lower central pressures, and higher precipitation rates. Grimley et al. (2024) used PGW simulations of TCs making landfall over North and South Carolina to show an increase of 65% of compound flooding and 0.8 m deeper flood depths under warmer and moister conditions.

1.4. Study Goals

The goal of this study is to analyze how extreme daily precipitation over Puerto Rico could change by mid-century under RCP8.5 given the island's vulnerability to rainfall extremes and climate change. We combine the advantages of high-resolution GCM simulations with those of CPMs by using the Model Prediction Across Scales-Atmosphere (MPAS-A; Skamarock et al., 2012). Discrete daily rainfall extremes are dynamically downscaled with MPAS-A during a historical (2001–2021) and future (2041–2061) period. This study represents new insights in future rainfall extremes by accounting for the dynamic and thermodynamic changes projected under future warming, while explicitly representing convection within the region of interest. We use these simulations to show how CPMs can provide additional details, particularly mesoscale processes, on future changes in rainfall extremes not fully represented by GCMs.

2. Methods

2.1. Identifying Extreme Rainfall Events

A 10-member ensemble of the high-resolution Community Earth System Model (MESACLIP) simulations from 1920 to 2100 is used to identify extreme rainfall events over Puerto Rico. The model has a 0.25° horizontal grid spacing for the atmosphere and land, while using 0.1° grid spacing for the ocean and ice (Chang et al., 2025). We select this model given its improved ability to capture mean rainfall over the central Caribbean (Martinez et al., 2025). The historical climate is simulated from 1920 to 2006 in all 10 ensemble members, except for the first member, which is a preindustrial run starting from 1850 and thus is excluded from our analysis. The future climate is simulated from 2006 to 2100 under the RCP8.5 emissions scenario.

The MESACLIP daily rainfall accumulation is spatially averaged over Puerto Rico to identify rainfall extremes from 2001 to 2021 and 2041–2061. We select a mid-century future time period to understand the more imminent changes to rainfall extremes in a warmer environment and use 2001–2021 as a recent historical period to compare with more robust high-resolution rainfall observations. Note that from 2006 to 2021, events are influenced by the emissions scenario RCP8.5 but this is expected to differ only slightly from historical emissions over this period.

In each of the 9 MESACLIP members, we first identify the 99th percentile of rainfall days (calculated including wet and dry days) separately for the historical and future period over Puerto Rico. Out of these, the top 3 rainfall events in the ERS from April–June and the top 4 events in the LRS from August–November are selected from each ensemble member given that the LRS is longer than the ERS and typically has more extreme rainfall days. This results in 63 extreme rainfall days in the historical climate, and 63 in the future (i.e., 7 days for each of the 9 members; Table 1) selected for simulations in MPAS. The ERS and LRS have different large-scale rainfall drivers over the Caribbean and thus are important to consider separately (Martinez et al., 2019), while also accounting for a majority of extreme rainfall days. Note that we do not consider the ∼20% of extreme rainfall days (above the 99th percentile) that fall outside of either the ERS or LRS.

We compare extremes of daily rainfall averaged over Puerto Rico in MESACLIP from 2001 to 2021 to observations in order to determine if the model can capture the general features of extreme rainfall. We select all rainfall amounts above the 99th percentile for the comparison, including both wet and dry days in our calculation, and choose the 99th percentile instead of a higher threshold in order to have a larger event sample size in the observations for a more robust evaluation. For observations, we use the Cooperative Observer Program (COOP) stations and the Integrated Multisatellite Retrievals for Global Precipitation (IMERG) data set. We select five COOP stations across Puerto Rico that have record lengths of at least 20 years for accurate comparison (Figure 1b). The IMERG data is a global gridded precipitation product at 0.1° × 0.1° and 30-min intervals

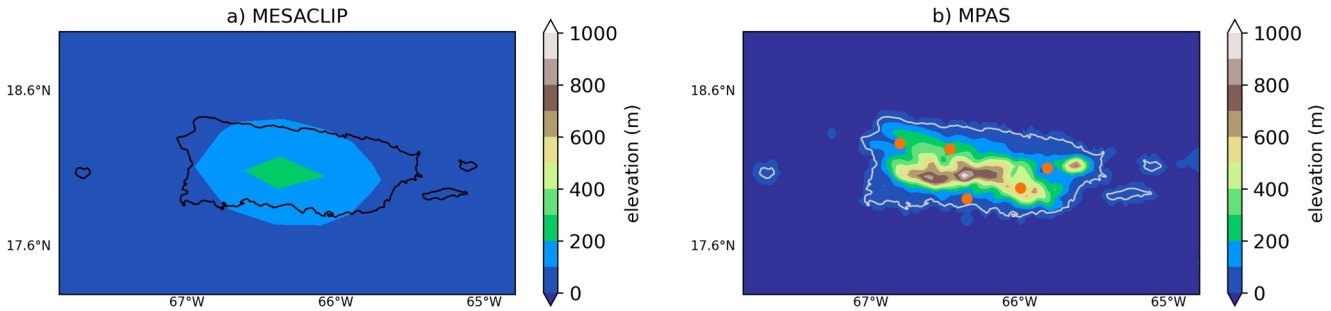

Figure 1. The topography over Puerto Rico as resolved by (a) the 0.25° MESACLIP data and (b) the 3-km grid-spacing in MPAS-A. The 5 orange circles show the locations of COOP stations used to validate the forcing data in representing rainfall extremes.

calibrated by the Global Precipitation Climatology Center (GPCC; Schneider et al., 2011) and we use the "Final" version 7 of IMERG (IMERG-F), which is for research purposes (Huffman et al., 2019).

Figure 2 shows the probability distribution function of the daily rainfall amounts above the 99th percentile in all 9 MESACLIP members from 2001 to 2021 compared to the COOP stations and the IMERG-F data set. The MESACLIP ensemble shows a low bias compared to observed rainfall extremes, with a mean of about 13 mm day^{-1} and maximum values up to 175 mm day^{-1}, whereas COOP and IMERG show a mean of ∼44 mm day^{-1} and maxima up to 175 mm day^{-1}. The low bias of MESACLIP is consistent with the underestimation of rainfall by climate models (Brotons et al., 2024; Martinez et al., 2025) and even ERA5 (Akinsanola et al., 2024) in this region, though this particular model was identified as performing better than others in the central Caribbean in terms of its mean rainfall, particularly in the ERS (Martinez et al., 2025). However, we find an underestimation of both mean and extreme rainfall over Puerto Rico using this data and caution interpretation in the results.

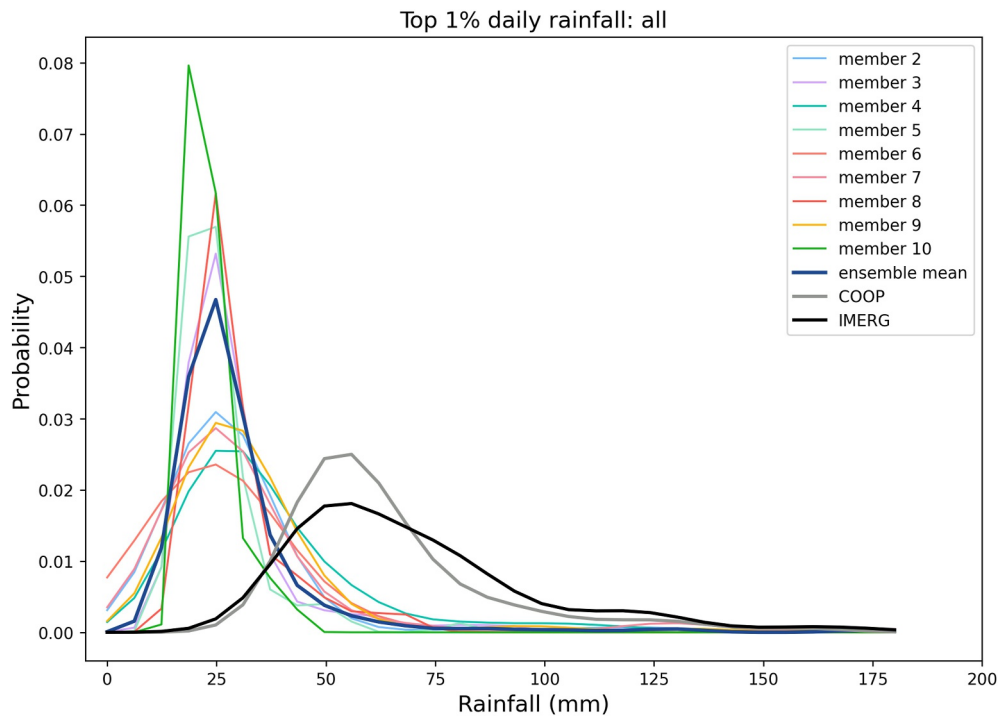

Figure 2. Probability density function of the top 1% of daily rainfall amounts from 2001 to 2021 averaged over Puerto Rico. The gray and black lines show observations from the average of the COOP stations shown in Figure 1 and IMERG-F, respectively. Colored lines show values from each of the 9 MESACLIP members, with the thick navy blue line showing the ensemble mean.

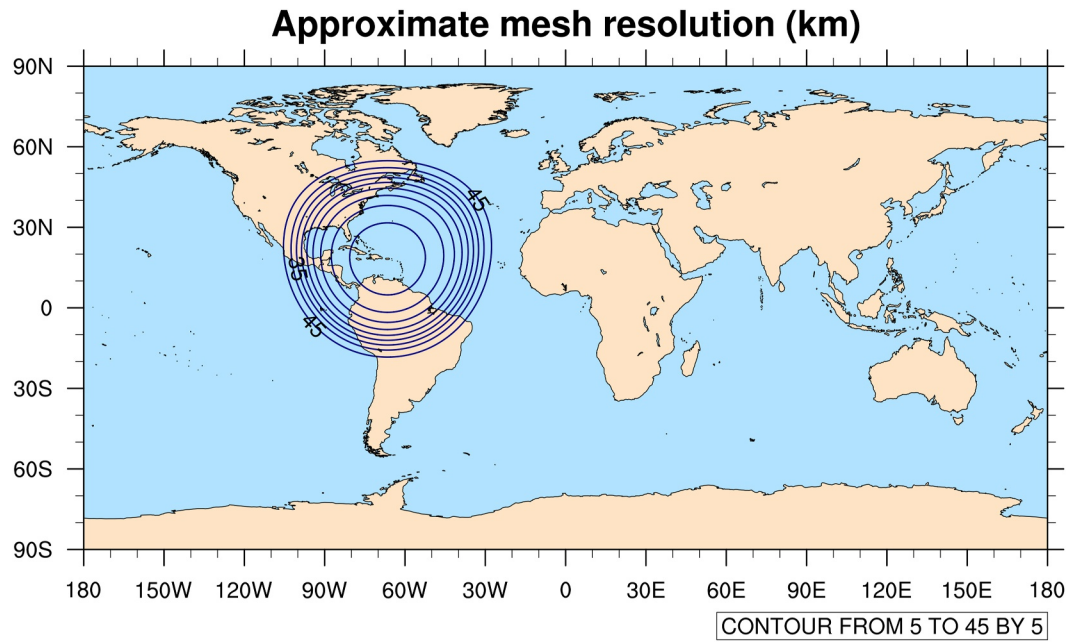

Figure 3. The MPAS-A model domain, with everything outside of the outer blue circle having a 60-km grid spacing and the circles showing the regional refinement from 60-km to 3-km in the inner circle, where Puerto Rico and surrounding Caribbean islands are located.

2.2. MPAS-A Set-Up

To capture more detailed changes to rainfall extremes over Puerto Rico, we use the Model Prediction Across Scales-Atmosphere (MPAS-A; Skamarock et al., 2012) model version 8.0.1. We use the 60–3 km circular mesh, where the inner domain over Puerto Rico and much of the Caribbean has a 3-km grid spacing and the grid gradually coarsens to 60-km over the rest of the world (Figure 3). By using this global MPAS configuration, we can seamlessly downscale the MESCALIP forcing data in a historial and future period to convection-permitting scales in a single model framework. Such a framework is necessary in order to capture the detailed topography of Puerto Rico and explicitly simulate deep moist convection, which are underresolved in MESACLIP (Figure 1). Based on this configuration, we use the "convection-permitting" physics suite which includes the scale-aware Grell-Freitas convection scheme (Grell & Freitas, 2014) for scales larger than 3-km, RRTMG shortwave and longwave radiation (Iacono et al., 2008), Xu-Randall subgrid cloud fraction (Xu & Randall, 1996), MYNN boundary-layer and surface-layer schemes (Nakanishi & Niino, 2004), Noah land-surface scheme (Niu et al., 2011), and Thompson microphysics (Thompson et al., 2008).

The MESACLIP 9-member ensemble was used to force MPAS-A at the initial time for individual extreme rainfall days during the historical and future climate. Some of the rainfall events were poorly simulated in MPAS, where rainfall rates were much weaker compared to the MESACLIP forcing data. This only occurred during the LRS, where 8 historical LRS events and 12 future LRS events failed to reproduce extreme precipitation, as defined by not reaching a threshold of 60% of the maximum rainfall accumulation produced by MESACLIP at any location over Puerto Rico. These cases were removed from the analysis and the day with the next highest rainfall amount that met the 99th percentile was downscaled and used. This resulted in 126 total simulations (63 historical and 63 future; Table 1).

Due to simulating individual events, we allowed for 12-hr of spin-up and 24 hr of simulations for a total of 36 hr simulations for each event. We conducted sensitivity tests of spin-up times and found that 12 hr was ideal for properly spinning up convection and not being too long for model drift of individual events (particularly TCs) to occur. Data was output hourly with 27 vertical pressure levels and regridded from the unstructured MPAS grid to approximately 3-km grid-spacing for analysis over Puerto Rico. Using the benefits of convection-permitting resolution in a global model allows us to understand how rainfall extremes are changing over Puerto Rico, while allowing for the full global changes to be simulated.

10.1029/2025EF007833

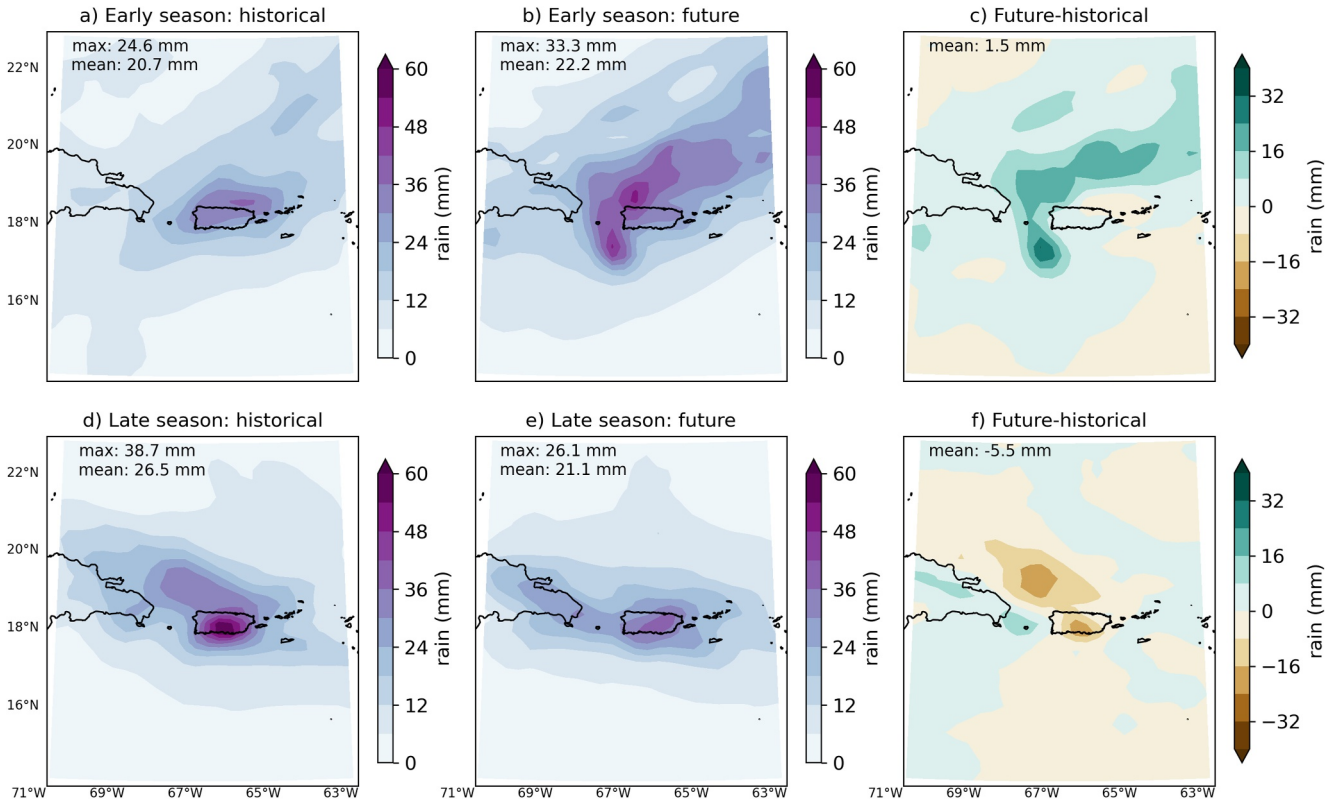

Figure 4. The ensemble average of extreme daily rainfall in MESACLIP, the forcing data, during (a) the early rainy season (ERS) from 2001 to 2021, (b) the ERS from 2041 to 2061, and (c) the difference between (b) and (a). The bottom row (d)–(f) is the same as (a)–(c) except for the late rainy season. Areas of increased future rainfall in (c), (f) are shown in greens and decreases are shown in browns. Values in the upper left corner show the ensemble area-average and maximum rainfall values over Puerto Rico and their changes.

2.3. TAMS Tracking Algorithm

The extreme rainfall events over Puerto Rico were classified based on using the Tracking Algorithm for Mesoscale Convection Systems (TAMS; Núñez Ocasio & Moon, 2024), which is an open source Python package. TAMS identifies MCSs based on cloud top temperatures ≤235 K with embedded cores of at most 219 K and with areas ≥4,000 km^2. These features were identified using the MPAS output, with areas meeting these definitions formed into polygons. TAMS tracks polygons using an area-overlapping threshold of 0.5 and backward linking. To specifically identify MCSs that affected Puerto Rico on extreme rainfall days, there must have been ≥3 MCSs of any duration or at least 1 MCS that existed ≥3 hr over the island. Isolated convection was based on there being <3 MCSs and no MCSs lasting >3 hr. Tropical cyclones (TCs) were identified through visual inspection and based on having at least 34-kt winds and spiral rainbands. Storms that did not fit the criteria for MCSs, isolated, convection, or TCs had unorganized stratiform rainfall, which only accounted for a handful of storms in the historical and future period, so results will not be shown. According to an intercomparison of MCS tracking algorithms, TAMS tends to produce relatively few large MCSs that are shorter lived than other trackers (Feng et al., 2024; Prein et al., 2024). It is possible that use of different tracking algorithms or criteria for determininge MCSs versus isolated storms could affect our results.

3. Results: Future Changes to Extreme Rainfall

3.1. Changes to Storm Rainfall

The MESACLIP rainfall on extreme rainfall days used to force MPAS during the ERS and LRS is shown in Figure 4. We show results as the mean over ensemble members and extreme rainfall days for each ensemble member, but note that individual ensemble members and events were used to force MPAS. During the historical ERS, there is a narrow region of extreme rainfall over Puerto Rico, with a mean (maximum) rainfall over the

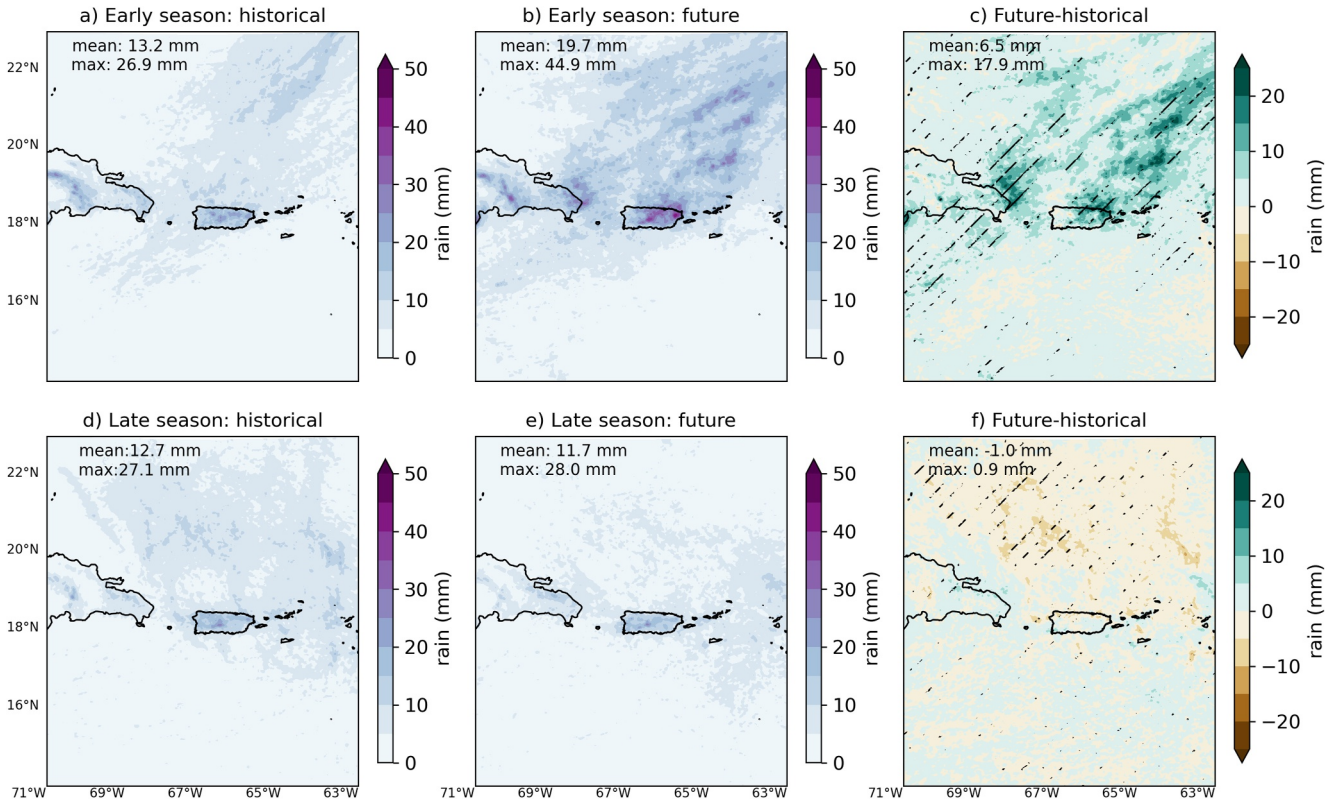

Figure 5. As in Figures 4a–4f but for MPAS simulations of extreme rainfall days. Hatched regions in (c) and (f) show locations where the future minus historical difference is statistically significant at 10% level after bootstrapping 1,000 times.

island of 20.7 mm (24.6 mm; Figure 4a). In the future ERS, the extreme rainfall increases in coverage and magnitude mainly west and north of the island (Figures 4b and 4c). The mean island rainfall increases by 1.5 mm (7.2%) in the future, with slight increases over most of the island (Figure 4c). In the historical LRS, the mean (maximum) rainfall is higher than the ERS at 26.5 mm (38.7 mm), with widespread rainfall over and north of Puerto Rico (Figure 4d). In the future LRS, the extreme rainfall is more zonally oriented, with mean (maximum) over the island decreasing to 21.1 mm (26.1 mm; Figure 4e). The future change in the LRS rainfall shows a complex pattern, with rainfall decreasing over and north of Puerto Rico and slight increases surrounding it. Overall, future LRS rainfall over Puerto Rico decreases on average by −5.5 mm (−20.8%; Figure 4f).

The extreme rainfall days from Figure 4 are downscaled in MPAS, which shows a few key differences compared to MESCALIP (Figure 5). First, the ensemble mean rainfall amounts are lower in MPAS during all seasons (Figures 5a, 5b, 5d, and 5e), though the maximum rainfall amounts are higher in MPAS except for the historical LRS (Figure 5d). In the ERS, area-average rainfall over Puerto Rico is 13.2 mm, compared to the 20.7 mm seen in MESACLIP (cf. Figure 5a vs. Figure 4a), with similarly lower amounts in the future ERS, historical LRS, and future LRS. The lower rainfall averages in MPAS does not mean that MPAS is failing to simulate higher rainfall intensities than MESACLIP, as MPAS shows localized areas of heavy rainfall compared to the broader rainfall amounts in MESACLIP's 0.25° resolution, which cannot properly resolve convection (Figure S1). This results in many grid cells over Puerto Rico with a rainfall accumulation of zero for a particular event, which results in a lower overall spatial average. Despite the lower rainfall averages, much more detail is seen in MPAS, with areas of localized maxima over Puerto Rico clearly distinguishable, unlike in MESACLIP.

While MPAS simulates increases in future extreme rainfall in the ERS and decreases in the LRS like MESACLIP, the magnitudes of the changes are different, with a 6.5 mm (49%) increase in the ERS and −1.0 mm (−7.9%) decrease in the LRS over Puerto Rico. The future increase in ERS rainfall is statistically significant at the 10% level over eastern Puerto Rico and to the northeast, as well as over the eastern part of Dominican Republic as shown by the hatched regions in Figure 5c based on bootstrapping with 1,000 iterations. The spatial pattern of

10.1029/2025EF007833

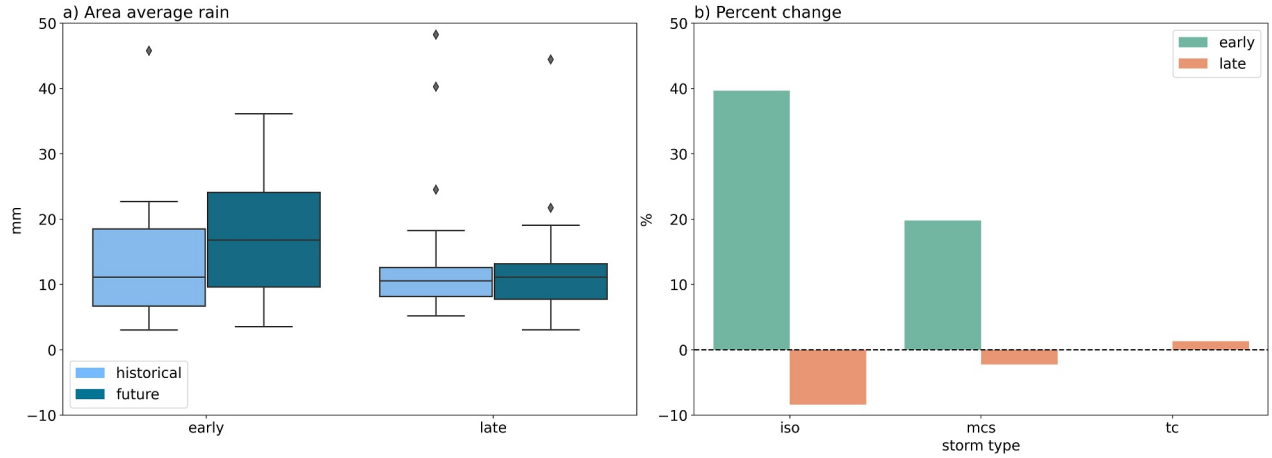

Figure 6. The spatially averaged extreme daily rainfall from MPAS over Puerto Rico during (a) the early rainy season (ERS) and late rainy season (LRS), and (b) the future percent change for different storm types where "iso" = isolated convection, "mcs" = mesoscale convective system, and "tc" = tropical cyclone. Boxplots show the 25th–75th percentile (Q1–Q3, which is the interquartile range [IQR]) of the ensemble in the box, the median as shown by the horizontal black line, whiskers show the minimum (Q1 – 1.5xIQR) and maximum (Q3 + 1.5xIQR), and diamonds represent outliers, where light blue boxplots show the historical values and dark blue boxplots show the future values. Storm types in (b) are divided into changes during the ERS (green) and LRS (orange).

increase during the ERS change is slightly different that in MESACLIP, with an increase in rainfall over eastern Puerto Rico and northeast of it (Figure 5c), unlike the more western and northern swath of increase in MESACLIP (Figure 4c). The LRS in MPAS shows areas of small increasing and decreasing rainfall like MESACLIP (Figure 5f vs. Figure 4f), though with less of a decrease over Puerto Rico. Only areas of decreasing rainfall are statistically significant in the LRS change, particularly to the north and south of Puerto Rico (Figure 5f).

While it is beyond the scope of this paper to corroborate whether MESCACLIP's or MPAS's future changes are more realistic in this region, the decrease in LRS extreme rainfall is similar to what has been observed in GCM projections of decreased mean and extreme precipitation over the Caribbean by 2100 for either annual or summer statistics (Almazroui et al., 2021; Brotons et al., 2024; Herrera et al., 2020; Pfahl et al., 2017). The projected increase in ERS extreme rainfall is in contrast to Bhardwaj et al. (2018), who finds reduced extreme hourly precipitation over Puerto Rico in June, July, and August by mid-century using 2-km simulations. This discrepancy could be due to a different climate model forcing and experimental design. Differences in the magnitude of change between MESACLIP's and MPAS's projections could be due to the different resolutions and consequently, processes that are captured at these finer resolutions. Given the benefit of MPAS in resolving convection and topography, we use these simulations to understand future changes to storm types over Puerto Rico.

Focusing on changes to rainfall extremes just over Puerto Rico, the historical area average rainfall during the ERS is 13.2 mm and increases to 19.7 mm in the future, which is a 49% increase (Figure 6a). During the LRS, the historical area average rainfall is 12.7 mm and decreases slightly in the future to 11.7 mm, which is a −7.9% decrease. This suggests that the ERS extreme precipitation may pose a greater risk in the future than it has in the past. Separating the rainfall changes by storm types in terms of % change (Figure 6b), increases in ERS rainfall are mainly driven by the 40% increase in rainfall from isolated convection, with a 20% increase from MCSs. In contrast, rainfall from isolated convection shows the largest decrease in the LRS of −8%, with a slight −2% decrease from MCS rainfall, and TCs being the only storm type with a slight increase of 2%. This suggests that most of the rainfall increases in the ERS and decreases in the LRS are being driven by changes in isolated convection, which are typically initiated through land-sea breezes and topography over the island (Jury et al., 2009).

Spatial plots of rainfall for different storm types and their changes are shown in Figures 7–9. For isolated convection, the unorganized and localized nature of rainfall over and surrounding Puerto Rico is apparent in the historical and future climate (Figure 7). The future change during the ERS shows that isolated rainfall increases nearly everywhere over the domain and is statistically significant at the 10% level after bootstrapping 1,000 times, particularly over eastern and southern Puerto Rico, with a mean increase of 3.1 mm (40%; Figure 7c). During the LRS, isolated rainfall shows areas of slight increases and decreases, with a mean decrease of −0.7 mm (−8%) and

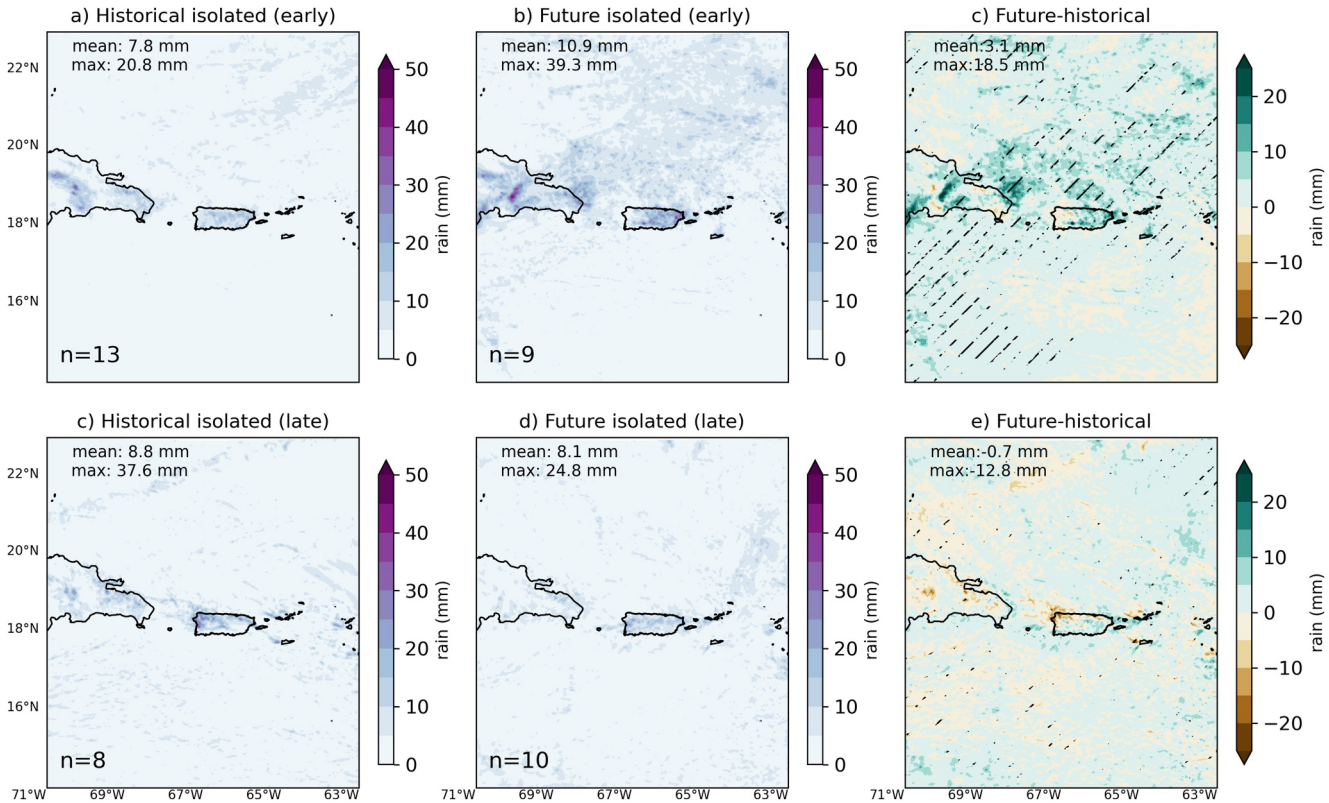

Figure 7. As in Figure 5, except for rainfall from isolated convection only. The "n" in the bottom right of each plot shows the number of events that went into each composite map.

localized increases over eastern Puerto Rico (Figure 6e). Relatively few areas show a statistically significant difference in the LRS isolated rainfall change, except for some areas of decreasing rainfall.

MCS rainfall shows a more organized and widespread rainfall pattern (Figure 8), with future rainfall changes in the ERS showing a quasi-linear southwest to northeast rainfall increase over northeastern Puerto Rico northwards and over eastern Dominican Republic (Figure 8c). During the ERS, area average MCS rainfall increases by 3.9 mm (20%) over Puerto Rico. Despite this large increase, there are few areas of stastically significant differences between the future and historical periods during the ERS. The LRS shows a −0.3 mm (−2%) decrease in MCS rainfall over Puerto Rico, with a particularly large decrease to the northeast of Puerto Rico, which is statistically significant. Over Puerto Rico, there are areas of slight increases and decreases (Figure 8e).

Despite having a small sample size of TCs in the extreme rainfall events ($n = 9$ for the historic period, $n = 6$ for the future), interesting patterns emerge in Figure 9. Historical TCs show a southeast to northwest path, with localized rainfall maxima over southern Puerto Rico and to the north of the island (Figure 9a). Future TCs show a more zonal pattern in their rainfall distribution, with rainfall maxima over central Puerto Rico largely following topography. The future change largely reflects the change in TC tracks, with a rainfall decrease to the north of Puerto Rico and increase to the east and south (Figure 9c). Both the rainfall decrease to the north and the rainfall increase to the southeast of Puerto Rico are statistically significant at the 10% level after bootstrapping 1,000 times. The area average TC rainfall change shows a 0.3 mm (1.6%) increase, with localized areas of increases over Puerto Rico, as the maximum rainfall increases by 13.5 mm. Though TCs in the current climate are associated with over half of the largest streamflow events (Hernández Ayala et al., 2017), these results suggest fewer TCs affect Puerto Rico by mid-century with possible changes in track that could potentially result in different locations being flooded in the future.

Overall, our results suggest an increasing risk of extreme rainfall by mid-century during the ERS and a slight reduction in extreme rainfall in the LRS. Extreme rainfall from isolated convective storms are the main contribution to the increase during the ERS and decrease in the LRS over Puerto Rico, with a secondary contribution

10.1029/2025EF007833

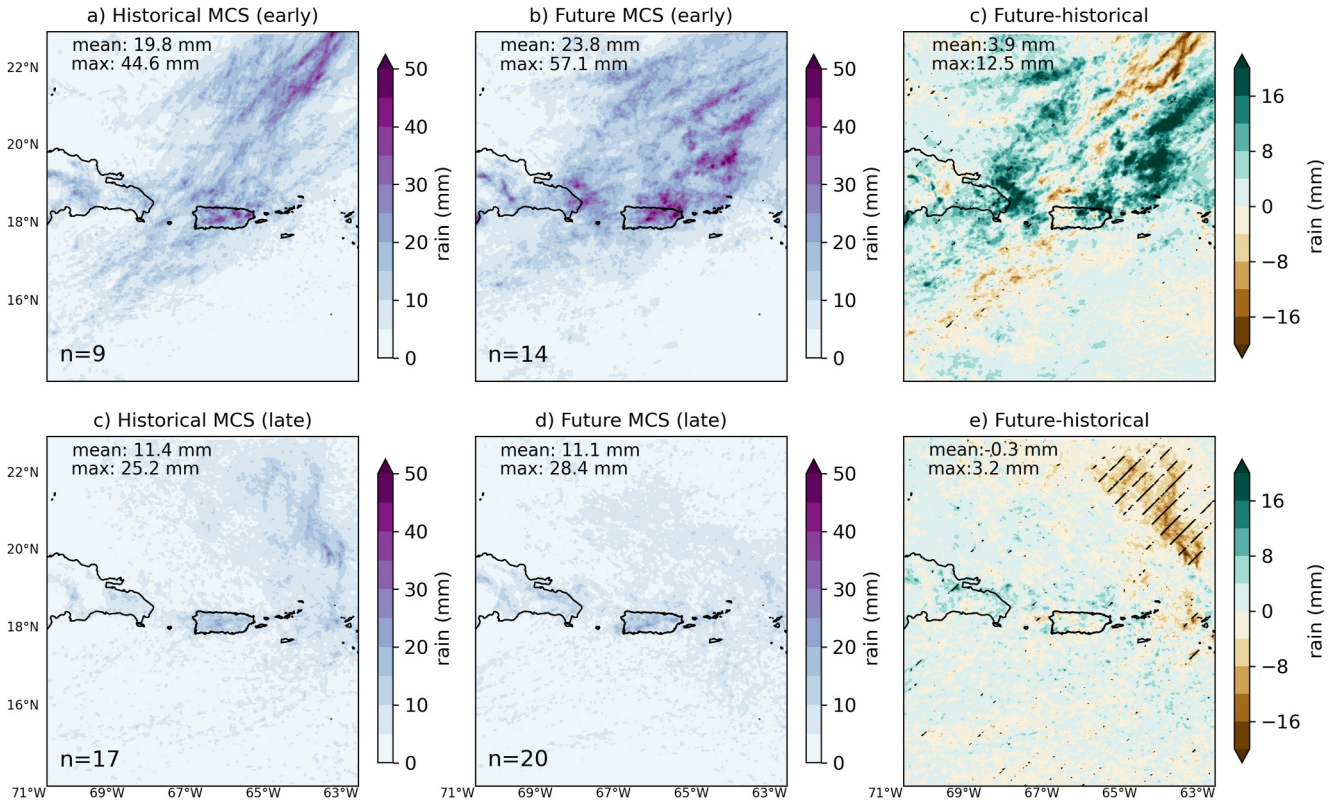

Figure 8. As in Figure 7, except for rainfall from mesoscale convective systems only.

from MCSs. Changes in TC rainfall show complex patterns, with a potential change in track in the future and slight rainfall increases over Puerto Rico, though the sample size is too small to draw robust conclusions.

3.2. Environmental Changes

Given the disparate changes in increasing rainfall extremes during the ERS and decreasing rainfall extremes in the LRS, we investigate future changes in large-scale and local-scale factors that could explain this difference using MESACLIP and MPAS. To understand the large-scale drivers in the background environment of extreme precipitation, we examine the change in monthly mean omega at 500 hPa during the ERS and LRS based on MESACLIP forcing data. Omega decreases (i.e., more upward motion) during the ERS in the future, with a decrease of −0.004 to −0.008 Pa/s over the Caribbean domain shown in Figure 10, which is statistically

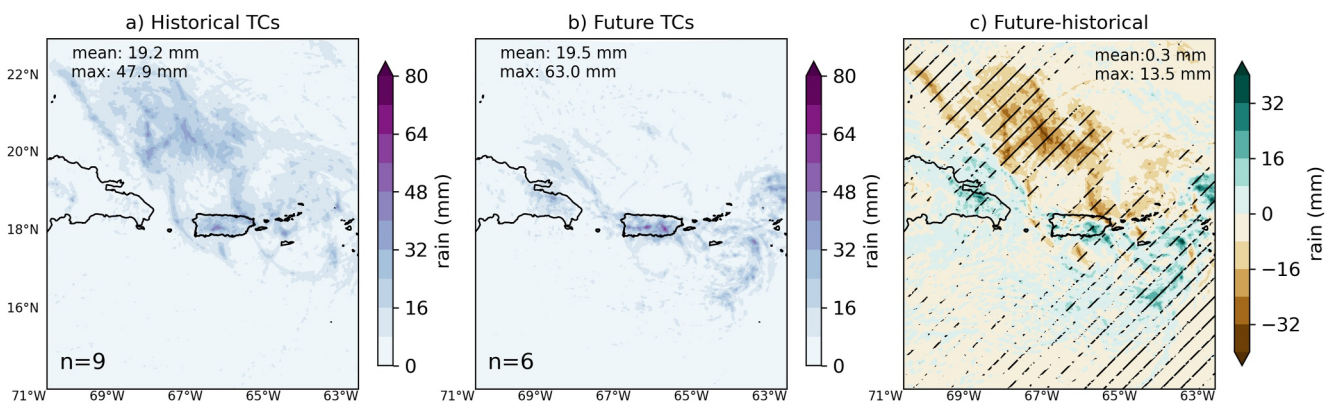

Figure 9. As in Figure 7, except for rainfall from Tropical cyclones (TCs) only. Note that we only look at rainfall from TCs in the late rainy season, as they do not occur in the early rainy season.

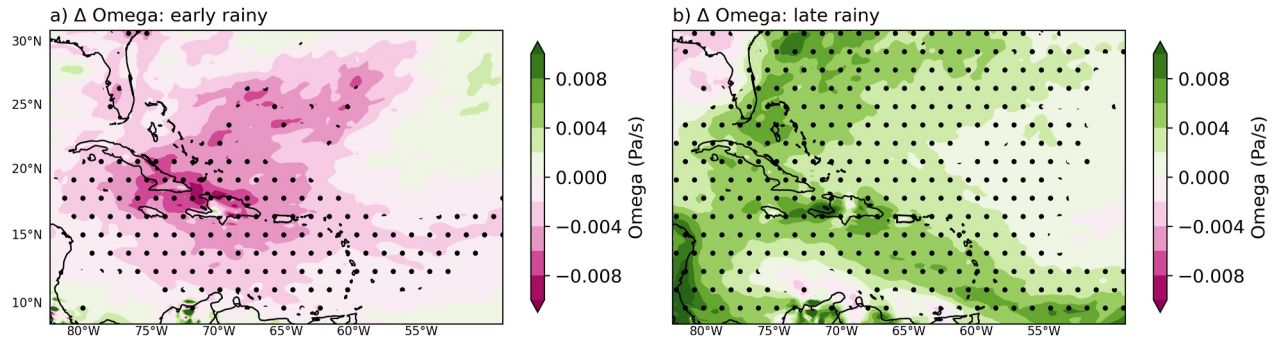

Figure 10. 500 hPa Ω averaged over (a) the early rainy season and (b) the late rainy season from the MESACLIP data. Areas of decreasing omega (upward motion) are shown in pink and increasing omega (downward motion) are shown in green. Dots indicate a statistically significant difference at $p < 0.05$ from a two-tailed *t*-test.

significant at the $p < 0.05$ level according to a two-tailed *t*-test (Figure 10a). In the LRS, omega significantly increases (i.e., more subsidence) over the Caribbean in the future by 0.004–0.008 Pa/s (Figure 10b). The future increasing upward motion during the ERS and increasing subsidence during the LRS is in line with the increasing rainfall during the ERS and rainfall reduction in the LRS. Brotons et al. (2024) found increasing subsidence and a consequent reduction in mean rainfall from May–November by 2100 over the Caribbean, which includes our LRS and part of our ERS. Brotons et al. (2024) attribute the increased subsidence in the future to warming sea surface temperatures in the eastern and central Pacific (thus changing to a more El-Niño like state) that weakens and shifts the Pacific Walker circulation and thus induces subsidence over the Caribbean. By considering the ERS and LRS separately, we show increasing subsidence in the LRS is consistent with the results from Brotons et al. (2024), but that omega changes differ in the ERS.

We also examine future changes in relative humidity (RH) profiles at the start of each extreme rainfall simulation given the impact that RH has on convective organization and precipitation efficiency (Doswell et al., 1996; Tobin

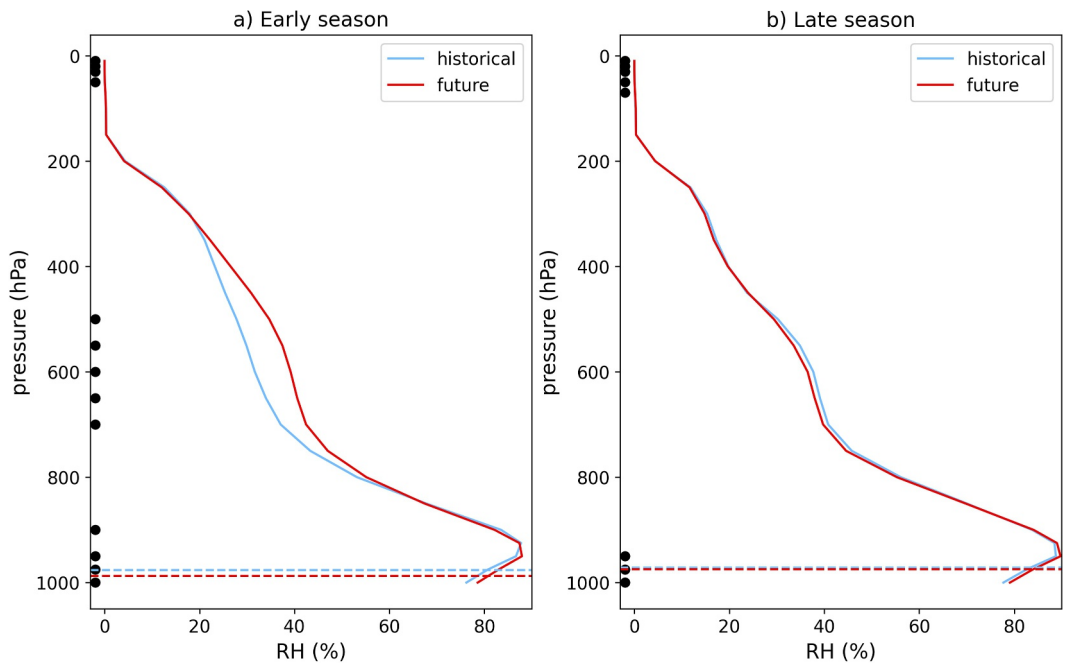

Figure 11. Vertical profiles of relatively humidity (RH) averaged over Puerto Rico at $t = 0$ in the MPAS simulations during (a) the early rainy season extreme rainfall days, and (b) the late rainy season extreme rainfall days. Red lines show values during the future simulations and blue lines show values during the historical simulations. Dashed lines show the lifting condensation levels and black dots show levels where the historical and future difference is significant ($p < 0.05$) according to a two-tailed *t*-test.

10.1029/2025EF007833

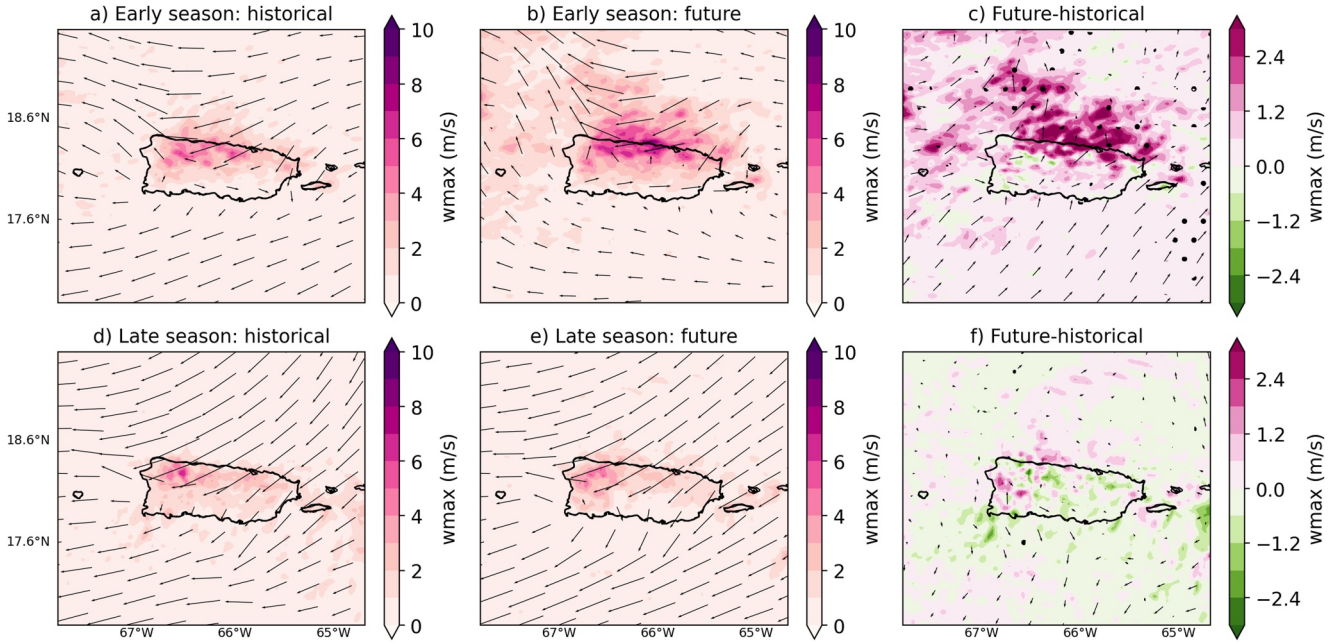

Figure 12. The average 925 hPa winds (vectors) and maximum daily updraft velocity (shading) during the extreme rainfall days simulated in MPAS in (a) the early rainy season (ERS) from 2001 to 2021, (b) the ERS from 2041 to 2061, and (c) the difference between (b) and (a) where pinks indicate stronger updrafts and greens indicate weaker updrafts. The bottom row (d)–(f) is the same as (a)–(c) except for the late rainy season.

et al., 2012; van der Drift & O'Gorman, 2025). RH at $t = 0$ in the MPAS simulations were averaged over Puerto Rico, which corresponds to the interpolated initial conditions from MESACLIP. These profiles were averaged over all extreme rainfall cases for the ERS and LRS. During the ERS, RH shows substantial moistening from the surface to 300 hPa in the future (red lines), with a lower lifting condensation level (LCL; dashed horizontal line), thus promoting greater rainfall efficiency (Figure 11a). This moistening is statistically significant according to a two-tailed t-test with $p < 0.05$ near the surface and from 700 hPa to 450 hPa. In the LRS, RH is nearly the same in the historical and future climate throughout much of the troposphere, except from 600 to 200 hPa, where the future RH is lower, though not significantly lower (Figure 11b).

For locally driven rainfall, sea breeze convergence and convective initiation over complex terrain play an important role over Puerto Rico (Bhardwaj et al., 2018; Jury & Chiao, 2013; Jury et al., 2009). To examine the role of local dynamics, the surface winds and maximum updraft velocity from MPAS after the 12-hr spin-up are examined in Figure 12. In the future, the surface winds show stronger convergence over northern Puerto Rico along the coastline during the ERS (Figure 12b) and consequently stronger maximum updrafts up to 2.4 ms^{-1} over the northern part of the island and northwards (Figure 12c). During the LRS, the surface winds show little change (Figure 12e), while maximum updrafts largely decrease over the island, with the exception of a slight increase in maximum updrafts over the far western part of the island (Figure 12f). This reduction in uplift, particularly orographic uplift, was seen by Bhardwaj et al. (2018) in their 20 years historical and future simualtions of Puerto Rico at 2-km grid spacing, which they attributed to reduced trade winds in the future. These local scale dynamics, which are important for generating rainfall extremes over Puerto Rico, cannot be seen using the coarser MESACLIP simulations (not shown) and thus provide a benefit for using MPAS to diagnose these changes.

The distinct changes by mid-century suggest that large-scale uplift, moistening, and local sea-breeze convergence and strong upward motion provides a favorable environment for the increasing intensity of rainfall extremes during the ERS. Conversely, the large-scale subsidence, mid-level drying, and weaker updrafts in the LRS provide a detrimental environment for the intensification of rainfall extremes in Puerto Rico.

4. Conclusions

126 simulations of daily rainfall extremes in a historic (2001–2021) and future (2041–2061) period were run using MPAS-A with 3-km grid-spacing over the Caribbean to understand changes to rainfall extremes over Puerto Rico.

These simulations provide a novel view of the impacts of future warming on rainfall extremes by running MPAS globally with a regional refinement over Puerto Rico, thus seamlessly downscaling coarser resolution initial conditions from MESACLIP while resolving convection and island topography. MPAS results show that by mid-century, the rainfall extremes will increase by 49% in the ERS and decrease by −8% in the LRS (Figure 5a). Future rainfall increases are larger in MPAS for the ERS compared to MESACLIP, while future rainfall decreases in the LRS in MPAS are smaller in magnitude than those projected by MESACLIP. However, MESACLIP cannot resolve convection (Figure S1) or the topography of Puerto Rico (Figure 1), so this is a major limitation of the forcing data that is improved by using MPAS.

The increase in ERS rainfall is driven by a 40% increase in rainfall from isolated convection and 20% increase from MCSs, while the decrease in LRS is mainly due to the −8% decrease in isolated convection and −2% decrease in MCS rainfall, despite the slight increase in rainfall from TCs (Figure 6b). This suggests extreme rainfall in the ERS becomes relatively more of a hazard in the future, particularly rainfall extremes from isolated convective storms. The future increase in ERS extreme rainfall is driven by the large-scale increasing upward motion, while increasing subsidence in the LRS over the Caribbean aids in reducing extreme rainfall (Figure 10). Increases in future subsidence seasonally over the Caribbean are a well-documented feature of warming (Bhardwaj et al., 2018; Brotons et al., 2024) and are associated with a weakening and shift of the Pacific Walker circulation (Brotons et al., 2024). The increased subsidence results in slight mid-level drying in the LRS over Puerto Rico, while the ERS shows substantial moistening (Figure 11). Local island effects show that in the future, there is more convergence along the populated northern coastline of Puerto Rico and stronger updrafts in the ERS (Figure 12c), while little changes in winds and a slight weakening of updrafts are seen in the LRS (Figure 12f). Therefore, both large-scale and local island effects due to warming are associated with the disparate changes in ERS and LRS extreme rainfall.

These simulations combine the advantages of convection-permitting and transient GCMs simulations, but have some limitations:

- Due to the high computational cost of running global simulations with a regional 3-km mesh, only 126 discrete rainfall events in a current and future climate could be simulated. While this captures the daily rainfall extremes based on MESACLIP output, the sample size of each storm type for the ERS and LRS in the historical and future simulations is limited. For example, TCs, which represent the primary hazard to Puerto Rico under current climate conditions (Hernández Ayala et al., 2017), are only present in 9 historical simulations and 6 future simulations, which makes it difficult to draw robust conclusions about the nature of their change.
- While MESACLIP performs better than other coarser GCMs over the Caribbean (Martinez et al., 2025), it still underestimates the magnitude of the top 1% of daily rainfall over Puerto Rico in compared to observations by ∼30 mm (Figure 2). This bias might underestimate the future rainfall change and should be kept in mind when interpreting results.
- In addition to inheriting the bias from MESACLIP, MPAS has its own biases. It produces lower mean rainfall amounts on the extreme rainfall days compared to MESACLIP, likely due to more locations have zero rainfall compared to MESACLIP. Locally, MPAS shows enhanced maximum rainfall over Puerto Rico, due to its ability to capture extreme convection rainfall (Figure S1). Given these biases, we caution interpretation of our results and suggest future studies look into improving the representation of rainfall extremes in the tropics in CPMs to better compare to observations.
- An additional caveat is that MESACLIP might not simulate extreme precipitation from all storm types similarly well, which would result in a biased sampling of events, and MPAS might intensify certain non-extreme precipitation conditions overproportionally, which are not sampled when only relying on MESACLIP output.
- MPAS struggled to simulate LRS extreme events, with 8 historical LRS events and 12 future LRS events thrown out due to underdoing rainfall compared to MESACLIP. This suggests MPAS might have issues properly capturing the highest rainfall producing events from TCs that occur during this time period. Thus caution is needed in comparing ERS and LRS rainfall amounts based on MPAS simulations.

Given the vulnerability of Puerto Rico to climate change, our results suggest that more consideration should be given to future ERS rainfall, given the increasing rainfall risk during this season compared to the LRS. Traditionally, much of the focus in studies and hazard mitigation is on the LRS due to the high-impact nature of TCs, like Hurricane Maria in 2017 (Pasch et al., 2018; Keellings & Hernández Ayala, 2019). While TC rainfall still

increases slightly in the future from these simulations and thus poses a future hazard, isolated convective rainfall during the ERS shows larger increases. Changes in the intensity of both ERS and LRS rainfall by mid-century could have large implications for agriculture, tourism, and hazard mitigation.

Conflict of Interest

The authors declare no conflicts of interest relevant to this study.

Availability Statement

COOP station data was downloaded from here: https://www.ncei.noaa.gov/products/land-based-station/cooperative-observer-network, while IMERG-F data was downloaded here: https://gpm.nasa.gov/data/directory. The latest version of MPAS-A can be downloaded via Github: https://github.com/MPAS-Dev/MPAS-Model. The MESACLIP data was downloaded from Castruccio et al. (2024a, 2024b).

Acknowledgments
This work is part of the MIT Climate Grand Challenge on Weather and Climate Extremes and was supported by MIT Climate Grand Challenges Subaward Agreement No. s5820. NCAR is a major facility sponsored by the National Science Foundation (NSF) under Cooperative Agreement 1852977. Thank you to Kelly Núñez Ocasio and Zachary Moon for help using TAMS and Abby Jaye for providing pre-processing tools for MESACLIP. We acknowledge high-performance computing via Derecho (https://doi.org/10.5065/qx9a-pg09) through the NSF NCAR Computational and Information Systems Laboratory and we thank Gretchen Mullendore for providing extra computational resources.

References

Adam, O., Schneider, T., & Brient, F. (2018). Regional and seasonal variations of the double-ITCZ bias in CMIP5 models. *Climate Dynamics*, *51*(1–2), 101–117. https://doi.org/10.1007/s00382-017-3909-1

Akinsanola, A. A., Jung, C., Wang, J., & Kotamarthi, V. R. (2024). Evaluation of precipitation across the contiguous United States, Alaska, and Puerto Rico in multi-decadal convection-permitting simulations. *Scientific Reports*, *14*(1), 1238. https://doi.org/10.1038/s41598-024-51714-3

Almazroui, M., Islam, M. N., Saeed, F., Saeed, S., Ismail, M., Ehsan, M. A., et al. (2021). Projected changes in temperature and precipitation over the United States, central America, and the Caribbean in CMIP6 GCMs. *Earth Systems and Environment*, *5*(1), 1–24. https://doi.org/10.1007/s41748-021-00199-5

Archer, L., Neal, J., Bates, P., Vosper, E., Carroll, D., Sosa, J., & Mitchell, D. (2024). Current and future rainfall-driven flood risk from hurricanes in Puerto Rico under 1.5 and 2°C climate change. *Natural Hazards and Earth System Sciences*, *24*(2), 375–396. https://doi.org/10.5194/nhess-24-375-2024

Bhardwaj, A., Misra, V., Mishra, A., Wootten, A., Boyles, R., Bowden, J. H., & Terando, A. J. (2018). Downscaling future climate change projections over Puerto Rico using a non-hydrostatic atmospheric model. *Climatic Change*, *147*(1–2), 133–147. https://doi.org/10.1007/s10584-017-2130-x

Brotons, M., Haarsma, R., Bloemendaal, N., De Vries, H., & Allen, T. (2024). Drivers of Caribbean precipitation change due to global warming: Analyses and emergent constraint of CMIP6 simulations. *Climate Dynamics*, *62*(5), 3395–3415. https://doi.org/10.1007/s00382-023-07072-3

Campbell, J. D., Taylor, M. A., Bezanilla-Morlot, A., Stephenson, T. S., Centella-Artola, A., Clarke, L. A., & Stephenson, K. A. (2021). Generating projections for the Caribbean at 1.5, 2.0 and 2.5°C from a high-resolution ensemble. *Atmosphere*, *12*(3), 328. https://doi.org/10.3390/atmos12030328

Castruccio, F., Chang, P., Danabasoglu, G., Fu, D., Rosenbloom, N., Zhang, Q., et al. (2024a). MESACLIP: A 10-member ensemble of CESM HR historical (1920-2005) simulations. *NSF National Center for Atmospheric Research*. https://doi.org/10.5065/7N1X-K278

Castruccio, F., Chang, P., Danabasoglu, G., Fu, D., Rosenbloom, N., Zhang, Q., et al. (2024b). MESACLIP: A 10-member ensemble of CESM HR RCP 8.5 (2006-2100) simulations. *NSF National Center for Atmospheric Research*. https://doi.org/10.5065/PNCR-5S34

Chang, P., Fu, D., Liu, X., Castruccio, F. S., Prein, A. F., Danabasoglu, G., et al. (2025). Enhancing global climate model resolution to improve extreme precipitation projections. *Nature*.

Chang, P., Zhang, S., Danabasoglu, G., Yeager, S. G., Fu, H., Wang, H., et al. (2020). An unprecedented set of high-resolution Earth system simulations for understanding multiscale interactions in climate variability and change. *Journal of Advances in Modeling Earth Systems*, *12*(12), e2020MS002298. https://doi.org/10.1029/2020MS002298

Doswell, C. A., Brooks, H. E., & Maddox, R. A. (1996). Flash flood forecasting: An ingredients-based methodology. *Weather and Forecasting*, *11*(4), 560–581. https://doi.org/10.1175/1520-0434(1996)011<0560:FFFAIB>2.0.CO;2

Feng, Z., Prein, A. F., Kukulies, J., Fiolleau, T., Jones, W. K., Maybee, B., et al. (2024). Mesoscale convective systems tracking method intercomparison (MCSMIP): Application to DYAMOND global km-scale simulations. *Preprints*. https://doi.org/10.22541/essoar.172405876.67413040/v1

Giannini, A., Chiang, J. C. H., Cane, M. A., Kushnir, Y., & Seager, R. (2001a). The ENSO teleconnection to the tropical Atlantic Ocean: Contributions of the remote and local SSTs to rainfall variability in the tropical americas. *Journal of Climate*, *14*(24), 4530–4544. https://doi.org/10.1175/1520-0442(2001)014<4530:TETTTT>2.0.CO;2

Giannini, A., Kushnir, Y., & Cane, M. A. (2000). Interannual variability of Caribbean rainfall, ENSO, and the Atlantic Ocean. *Journal of Climate*, *13*(2), 297–311. https://doi.org/10.1175/1520-0442(2000)013<0297:IVOCRE>2.0.CO;2

Giannini, A., Kushnir, Y., & Cane, M. A. (2001b). Seasonality in the impact of ENSO and the north Atlantic high on Caribbean rainfall. *Physics and Chemistry of the Earth - Part B: Hydrology, Oceans and Atmosphere*, *26*(2), 143–147. https://doi.org/10.1016/S1464-1909(00)00231-8

Grell, G. A., & Freitas, S. R. (2014). A scale and aerosol aware stochastic convective parameterization for weather and air quality modeling. *Atmospheric Chemistry and Physics*, *14*(10), 5233–5250. https://doi.org/10.5194/acp-14-5233-2014

Grimley, L. E., Hollinger Beatty, K. E., Sebastian, A., Bunya, S., & Lackmann, G. M. (2024). Climate change exacerbates compound flooding from recent tropical cyclones. *Npj Natural Hazards*, *1*(1), 45. https://doi.org/10.1038/s44304-024-00046-3

Gutmann, E. D., Rasmussen, R. M., Liu, C., Ikeda, K., Bruyere, C. L., Done, J. M., et al. (2018). Changes in hurricanes from a 13-Yr convection-permitting pseudo–global warming simulation. *Journal of Climate*, *31*(9), 3643–3657. https://doi.org/10.1175/JCLI-D-17-0391.1

Heim, C., Leutwyler, D., & Schär, C. (2023). Application of the Pseudo-Global warming approach in a kilometer-resolution climate simulation of the tropics. *Journal of Geophysical Research: Atmospheres*, *128*(5), e2022JD037958. https://doi.org/10.1029/2022JD037958

Hernández Ayala, J. J., Keellings, D., Waylen, P. R., & Matyas, C. J. (2017). Extreme floods and their relationship with tropical cyclones in Puerto Rico. *Hydrological Sciences Journal*, *62*(13), 2103–2119. https://doi.org/10.1080/02626667.2017.1368521

Herrera, D. A., Mendez-Tejeda, R., Centella-Artola, A., Martínez-Castro, D., Ault, T., & Delanoy, R. (2020). Projected hydroclimate changes on Hispaniola Island through the 21st century in CMIP6 models. *Atmosphere*, *12*(1), 6. https://doi.org/10.3390/atmos12010006

Hersbach, H., Bell, B., Berrisford, P., Hirahara, S., Horányi, A., Muñoz-Sabater, J., et al. (2020). The ERA5 global reanalysis. *Quarterly Journal of the Royal Meteorological Society*, *146*(730), 1999–2049. https://doi.org/10.1002/qj.3803

Hosannah, N., González, J. E., Lunger, C., & Niyogi, D. (2019). Impacts of local convective processes on rain on the Caribbean Island of Puerto Rico. *Journal of Geophysical Research: Atmospheres*, *124*(12), 6009–6026. https://doi.org/10.1029/2018JD029825

Huffman, G. J., Stocker, E. F., Bolvin, D. T., Nelkin, E. J., & Tan, J. (2019). GPM IMERG final precipitation L3 1 day 0.1 degree x 0.1 degree V06 [Dataset]. In A. Savtchenko (Ed.). Goddard Earth Sciences Data and Information Services Center (GES DISC). https://doi.org/10.5067/GPM/IMERGDF/DAY/06

Iacono, M. J., Delamere, J. S., Mlawer, E. J., Shephard, M. W., Clough, S. A., & Collins, W. D. (2008). Radiative forcing by long-lived greenhouse gases: Calculations with the AER radiative transfer models. *Journal of Geophysical Research*, *113*(D13), 2008JD009944. https://doi.org/10.1029/2008JD009944

Jury, M. R. (2009). An intercomparison of observational, reanalysis, satellite, and coupled model data on mean rainfall in the Caribbean. *Journal of Hydrometeorology*, *10*(2), 413–430. https://doi.org/10.1175/2008JHM1054.1

Jury, M. R. (2018). Puerto Rico sea level trend in regional context. *Ocean and Coastal Management*, *163*, 478–484. https://doi.org/10.1016/j.ocecoaman.2018.08.006

Jury, M. R., & Chiao, S. (2013). Leeside boundary layer confluence and afternoon thunderstorms over mayaguez, Puerto Rico. *Journal of Applied Meteorology and Climatology*, *52*(2), 439–454. https://doi.org/10.1175/JAMC-D-11-087.1

Jury, M. R., Chiao, S., & Harmsen, E. W. (2009). Mesoscale structure of trade wind convection over Puerto Rico: Composite observations and Numerical Simulation. *Boundary-Layer Meteorology*, *132*(2), 289–313. https://doi.org/10.1007/s10546-009-9393-3

Keellings, D., & Hernández Ayala, J. J. (2019). Extreme rainfall associated with hurricane maria over Puerto Rico and its connections to climate variability and change. *Geophysical Research Letters*, *46*(5), 2964–2973. https://doi.org/10.1029/2019GL082077

Kendon, E. J., Roberts, N. M., Fowler, H. J., Roberts, M. J., Chan, S. C., & Senior, C. A. (2014). Heavier summer downpours with climate change revealed by weather forecast resolution model. *Nature Climate Change*, *4*(7), 570–576. https://doi.org/10.1038/nclimate2258

Martin, E. R., & Schumacher, C. (2011). The Caribbean low-level jet and its relationship with precipitation in IPCC AR4 models. *Journal of Climate*, *24*(22), 5935–5950. https://doi.org/10.1175/JCLI-D-11-00134.1

Martinez, C., Goddard, L., Kushnir, Y., & Ting, M. (2019). Seasonal climatology and dynamical mechanisms of rainfall in the Caribbean. *Climate Dynamics*, *53*(1–2), 825–846. https://doi.org/10.1007/s00382-019-04616-4

Martinez, C. J., Simpson, I. R., Fasullo, J. T., & Prein, A. F. (2025). An evaluation of the seasonal Caribbean hydroclimate in low and high-resolution CESM and other CMIP6 models. *Climate Dynamics*, *63*(1), 33. https://doi.org/10.1007/s00382-024-07516-4

Nakanishi, M., & Niino, H. (2004). An improved mellor–yamada Level-3 model with condensation physics: Its design and verification. *Boundary-Layer Meteorology*, *112*(1), 1–31. https://doi.org/10.1023/B:BOUN.0000020164.04146.98

Niu, G.-Y., Yang, Z.-L., Mitchell, K. E., Chen, F., Ek, M. B., Barlage, M., et al. (2011). The community Noah land surface model with multiparameterization options (Noah-MP): 1. Model description and evaluation with local-scale measurements. *Journal of Geophysical Research*, *116*(D12), D12109. https://doi.org/10.1029/2010JD015139

Núñez Ocasio, K. M., & Dougherty, E. M. (2024). The effect of pseudo-global warming on the weather-climate system of Africa in a convection-permitting model. *Geophysical Research Letters*, *51*(24), e2024GL112341. https://doi.org/10.1029/2024GL112341

Núñez Ocasio, K. M., & Moon, Z. L. (2024). TAMS: A tracking, classifying, and variable-assigning algorithm for mesoscale convective systems in simulated and satellite-derived datasets. *Geoscientific Model Development*, *17*(15), 6035–6049. https://doi.org/10.5194/gmd-17-6035-2024

O'Connor, J. E., & Costa, J. E. (2004). Spatial distribution of the largest rainfall-runoff floods from basins between 2.6 and 26,000 km^2 in the United States and Puerto Rico. *Water Resources Research*, *40*(1), 2003WR002247. https://doi.org/10.1029/2003WR002247

Pasch, R. J., Penny, A. B., & Berg, R. (2018). Hurricane Maria (AL152017). In *National Hurricane Center tropical cylcone report*. Retrieved from https://www.nhc.noaa.gov/data/tcr/AL152017_Maria.pdf

Patricola, C. M., & Wehner, M. F. (2018). Anthropogenic influences on major tropical cyclone events. *Nature*, *563*(7731), 339–346. https://doi.org/10.1038/s41586-018-0673-2

Pfahl, S., O'Gorman, P. A., & Fischer, E. M. (2017). Understanding the regional pattern of projected future changes in extreme precipitation. *Nature Climate Change*, *7*(6), 423–427. https://doi.org/10.1038/nclimate3287

Prein, A. F., Feng, Z., Fiolleau, T., Moon, Z. L., Núñez Ocasio, K. M., Kukulies, J., et al. (2024). Km-Scale simulations of mesoscale convective systems over South America—A feature tracker intercomparison. *Journal of Geophysical Research: Atmospheres*, *129*(8), e2023JD040254. https://doi.org/10.1029/2023JD040254

Prein, A. F., Langhans, W., Fosser, G., Ferrone, A., Ban, N., Goergen, K., et al. (2015). A review on regional convection-permitting climate modeling: Demonstrations, prospects, and challenges. *Reviews of Geophysics*, *53*(2), 323–361. https://doi.org/10.1002/2014RG000475

Prein, A. F., Mooney, P. A., & Done, J. M. (2023). The mutli-scale interactiosn of atmospheric phenomenon in mean and extreme precipitation. *Earth's Future*, *11*(11), 1–22. https://doi.org/10.1029/2023EF003534

Schär, C., Frei, C., Lüthi, D., & Davies, H. C. (1996). Surrogate climate-change scenarios for regional climate models. *Geophysical Research Letters*, *23*(6), 669–672. https://doi.org/10.1029/96GL00265

Schneider, U., Becker, A., Finger, P., Meyer-Christoffer, A., Rudolf, B., & Ziese, M. (2011). GPCC Full Data Reanalysis Version 6.0 at 0.5°: Monthly Land-Surface Precipitation from Rain-Gauges built on GTS-based and Historic Data. https://doi.org/10.5676/DWD_GPCC/FD_M_V6_050

Skamarock, W. C., Klemp, J. B., Duda, M. G., Fowler, L. D., Park, S.-H., & Ringler, T. D. (2012). A multiscale nonhydrostatic atmospheric model using centroidal voronoi tesselations and C-Grid staggering. *Monthly Weather Review*, *140*(9), 3090–3105. https://doi.org/10.1175/MWR-D-11-00215.1

Small, R. J., Bacmeister, J., Bailey, D., Baker, A., Bishop, S., Bryan, F., et al. (2014). A new synoptic scale resolving global climate simulation using the Community Earth System Model. *Journal of Advances in Modeling Earth Systems*, *6*(4), 1065–1094. https://doi.org/10.1002/2014MS000363

Thomas, A., Shooya, O., Rokitzki, M., Bertrand, M., & Lissner, T. (2019). Climate change adaptation planning in practice: Insights from the Caribbean. *Regional Environmental Change*, *19*(7), 2013–2025. https://doi.org/10.1007/s10113-019-01540-5

Thompson, G., Field, P. R., Rasmussen, R. M., & Hall, W. D. (2008). Explicit forecasts of Winter precipitation using an improved bulk microphysics scheme. Part II: Implementation of a new snow parameterization. *Monthly Weather Review*, *136*(12), 5095–5115. https://doi.org/10.1175/2008MWR2387.1

Tobin, I., Bony, S., & Roca, R. (2012). Observational evidence for relationships between the degree of aggregation of deep convection, water vapor, surface fluxes, and radiation. *Observational Evidence for Relationships between the Degree of Aggregation of Deep Convection, Water Vapor, Surface Fluxes, and Radiation*, *25*(20), 6885–6904. https://doi.org/10.1175/JCLI-D-11-00258.1

van der Drift, R. J., & O'Gorman, P. A. (2025). Dependence of convective precipitation extremes on near-surface relative humidity. *Journal of Climate*, *38*(21), 6207–6225. https://doi.org/10.1175/JCLI-D-24-0738.1

Xu, K.-M., & Randall, D. (1996). A semiempirical cloudiness parameterization for use in climate models. *Journal of the Atmospheric Sciences*, *53*(21), 3084–3101. https://doi.org/10.1175/1520-0469(1996)053<3084:ascpfu>2.0.co;2

Zhang, X., Liu, H., & Zhang, M. (2015). Double ITCZ in coupled ocean-atmosphere models: From CMIP3 to CMIP5: Double ITCZ in CMIP3 and CMIP5 aogcms. *Geophysical Research Letters*, *42*(20), 8651–8659. https://doi.org/10.1002/2015GL065973